

# Colorimetric and Photometric Modeling of Liquid Crystal Displays

Louis D. Silverstein  
VCD Sciences, Inc.  
9695 East Yucca Street, Scottsdale, AZ 85260

Thomas G. Fiske  
Xerox Palo Alto Research Center  
3333 Coyote Hill Road, Palo Alto, CA 94304

## Introduction

Liquid crystal displays (LCDs) are currently the leading candidate technology for the next generation of high-performance color workstations. Color LCD technology has been maturing at a rapid pace along with major improvements in display performance. This is at least in part due to large research and development expenditures focused on bringing color LCD technology to market. LCDs offer the extraordinary design flexibility of a light valve based device, while exhibiting the desirable characteristics of relatively low volume, weight, and power consumption. Moreover, with proper optimization of optical and electronic components, color LCDs are capable of color performance equal to or exceeding that of the venerable shadow-mask color CRT.

For a color CRT, the spectral composition and intensity of emitted light is a function of the excitation of phosphors by a stream of electrons emitted by a cathode. Since the intensity of emissions from each of the three primary color phosphors (R, G, and B) is directly proportional to the beam current while the spectral composition of the emission from each phosphor is invariant across beam current, the color and luminance of the color CRT are simply related to the luminous proportions of emitted light from each of the three primary color phosphors. There are generally no active optical elements involved, and the spectral composition of the output of the color CRT can be considered to be isotropic as well as homogenous across space and time. Thus, assuming that the spectral power distribution of the emissions from the R, G and B phosphors are known and suitably converted to tristimulus values (e.g. via the CIE 2° color matching functions), the colorimetric and photometric performance of the CRT may be readily characterized and optimized in tristimulus space.

Unlike the color CRT, which is optically simple and thus relatively easy to model and optimize in terms of colorimetric/photometric performance, the color LCD is optically complex. A transmissive color LCD is composed of a source of illumination and a multitude of layered optical elements which each modify the spectral composition of light originating from the source. Moreover, some of these elements, such as polarizers, retardation films and the liquid crystal (LC) layer itself, are optically anisotropic and birefringent layers which produce complex spectral modifications that vary as a function of the material parameters and construction of the LC cell, display voltage (i.e., luminance or gray level), and the direction of light propagation.

It should be apparent that the colorimetric modeling and optimization of an LCD is a much more complex task than comparable analyses for a color CRT. In this paper we describe the foundations of LCD operation, including some basics of LCD optical models and the effects of various LCD design parameters on the spectral, intensive, and angular propagation of light through an LCD. Further, we present a method for estimating the colorimetric and photometric characteristics of color LCDs which enables the investigation of the effects of variations in a number of critical color LCD components (e.g., spectral power distribution of the source of illumination, color filter dye concentration and thickness, LC birefringence, and LCD cell construction geometry) on the ultimate chromaticity and luminance rendering capabilities of the display. Finally, we present both modeled and empirical data on the color performance of today's state-of-the-art color LCDs, compare this performance with that of existing color CRTs, and discuss the promises and problems of this new generation of high-performance color imaging devices.

# Fundamentals of Color LCD Operation

## Some Basic Concepts of Liquid Crystals

Liquid crystals are complex, anisomeric organic molecules which, under certain temperature conditions, exhibit the fluid characteristics of a liquid and the molecular orientational order characteristics of a solid.<sup>1</sup> A consequence of the ordering of anisomeric molecules is that LCs exhibit mechanical, electric, magnetic and optical anisotropy.<sup>2,3</sup> There are many different types of LCs and display optical configurations to take advantage of their unique optical characteristics. It is important to recognize that most LC materials are uniaxial and birefringent. Uniaxial materials possess one unique axis, the optic axis, which is parallel to the liquid crystal director (i.e., the long axis of the molecules). The anisotropic nature of LC materials gives them the optical property of birefringence, which refers to the phenomenon of light traveling with different velocities in crystalline materials depending on the propagation direction and the orientation of the light polarization relative to the crystalline axes.<sup>2</sup> For a uniaxial LC, this implies different dielectric constants and refractive indices for the unique or "extraordinary" direction and for other "ordinary" directions in the LC material. The most widely used LC phase is the nematic type, which is shown Figure 1 along with its principle axes and associated dielectric and optical parameters.<sup>4</sup>

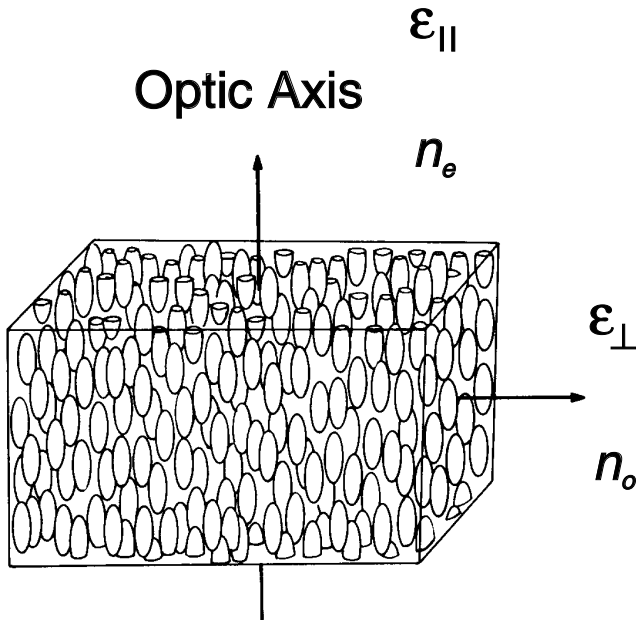


**Figure 1.** Nematic LC with principal axes and associated dielectric and optical parameters

Definitions of the basic parameters which determine the electrical and optical performance of the LC are provided in Equation (1), which also describes the phase difference between polarization components produced by the birefringence and path length through the LC layer.<sup>3,4</sup>

For a positive uniaxial material

$$\Delta = \epsilon_{\parallel} - \epsilon_{\perp}$$

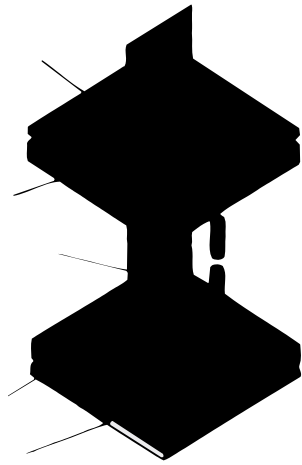
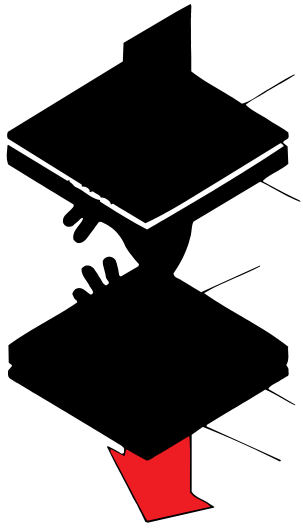
$$\Delta n = n_e - n_o$$

$$P_d = \frac{2\pi \Delta n d}{\lambda}$$

Where:

- $\epsilon_{\parallel}$  = dielectric constant  $\parallel$  to the LC director
- $\epsilon_{\perp}$  = dielectric constant  $\perp$  to the LC director
- $n_e$  = refractive index  $\parallel$  to the LC director
- $n_o$  = refractive index  $\perp$  to the LC director
- $\Delta$  = dielectric anisotropy
- $\Delta n$  = birefringence
- $\lambda$  = wavelength
- $d$  = LC layer thickness
- $P_d$  = phase difference of polarization components

The predominant LC cell configuration for high-performance color LCDs is the twisted-nematic cell. In the TN cell, incoming light is initially linearly polarized by an entrance polarizer and then the axis of polarization is optically rotated by the LC layer. The typical twist or rotation angle used for most TN LCDs is 90°, although other twist angles may be used to achieve certain desired optical characteristics.<sup>3</sup> After optical rotation by the LC layer, the polarization state of light exiting the LC layer is analyzed by the exit polarizer or "analyzer." Two principle configurations of TN cell entrance and exit polarizers are used, LCDs that utilize crossed polarizers are often called normally-white (NW) mode LCDs while those consisting of parallel polarizers are typically called normally-black (NB) mode LCDs. Figure 2 illustrates the basic principles of operation of a TN cell operated in the NW mode.



Properties for three of the optical components of the color LCD will have the principle effects on the ultimate colorimetric and photometric characteristics of the display: the spectral power distribution (SPD) of the illumination source; the spectral transmission of the thin-film color selection filters; and the selection of the LC material and tuning of the LC cell gap.<sup>7</sup> Here we consider aspects the spectral tuning of each of these elements.

Most direct-view color LCDs utilize either hot-cathode (HCF) or cold-cathode (CCF) fluorescent lamps for backlight illumination. Tri-band phosphor mixtures are typically employed to improve color performance for these lamps. For a tri-band HCF or CCF source, a variety of color phosphors can be utilized and then the SPD of the lamp can be tuned approximately by the following simple relations:<sup>7</sup>

$$S_{src}(\lambda) = P_r S_r(\lambda) + P_g S_g(\lambda) + P_b S_b(\lambda) + S_{ml}(\lambda)$$

Where:

$S_{src}$  = SPD of the source

$S_r(\lambda)$  = SPD of the R component

$S_g(\lambda)$  = SPD of the G component

$S_b(\lambda)$  = SPD of the B component

$S_{ml}(\lambda)$  = SPD of the visible mercury lines

$P_x$  = Proportion of R, G, or B component

Direct-view color LCDs typically utilize thin-film color absorption filters to accomplish primary color selection. The variety of dyes and pigments which are compatible with LC materials and the LCD manufacturing process are limited. Thus, there are limited degrees of freedom for tailoring the spectral transmission of thin-film color filters. Once the particular filter materials are selected, filter thickness and dye concentration can be adjusted within a range compatible with thin-film deposition processes. If the spectral transmission of a set of reference filter materials is known, and the dye or pigment in concentration is known to follow Beer's Law within the range of concentrations used, then the spectral transmission of the filter material at other dye concentrations and film thicknesses may be estimated via the use of the Beer-Lambert Law as follows:<sup>7,8</sup>

$$T_r(\lambda) = T_{r-ref}(\lambda)^\gamma$$

$$T_g(\lambda) = T_{g-ref}(\lambda)^\gamma$$

$$T_b(\lambda) = T_{b-ref}(\lambda)^\gamma$$

Where:

$$T_{x-ref}(\lambda) = \text{trans. of reference R, G, or B filter} \quad (3)$$

$$d_{x-ref} = \text{dye conc. of ref. R, G, or blue filter}$$

$$t_{x-ref} = \text{thickness of ref. R, G, or B filter}$$

$$d_x = \text{desired dye conc. of R, G, or B filter}$$

$$t_x = \text{desired thickness of R, G, or B filter}$$

$$\gamma = (d_x/d_{x-ref}) (t_x/t_{xref})$$

The design trade-offs for adjusting color filter thickness and/or dye concentration will, of course, be a change in the light throughput efficiency of the LCD.

The LC cell gap is a critical parameter for tuning the color performance, luminance and contrast ratio of a color LCD.<sup>6,7</sup> As mentioned in the previous section, for any given LC birefringence and LC cell gap, maxima and minima of cell transmission can only be achieved at a specific series of discrete wavelengths. The cell gap may be selected such that LCD contrast ratio, color gamut or color saturation are maximized or according to some weighted combination of display metrics. Figure 4 illustrates the effects of varying the cell gap on the transmission of the on- and off-states of a binary LCD. We have assumed ideal polarization to emphasize transmission variation with wavelength, and only the optically active state for each mode is shown.

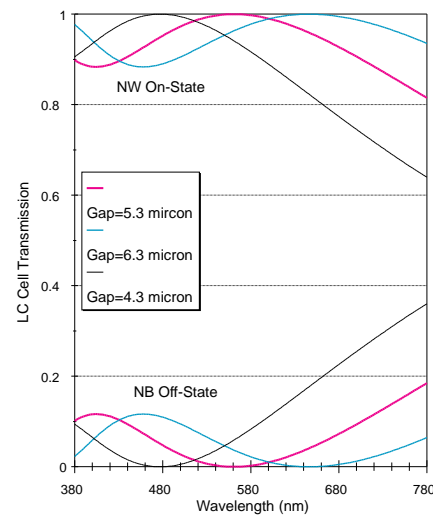


**Figure 4.** LC cell transmission as a function of wavelength and cell gap

The following set of equations may be used to determine the spectral tuning characteristics of the LC layer for a binary color LCD viewed on-axis:<sup>6,7</sup>

For the NB mode:

$$T_{lc-off}(\lambda) = \frac{\sin^2[\theta(1+u^2)^{1/2}]}{(1+u^2)} + T_{xp}(\lambda)$$

$$T_{lc-on}(\lambda) = \sin^2\theta$$

For the NW Mode:

$$T_{lc-off}(\lambda) = 1 - (\sin^2\theta) + T_{xp}(\lambda)$$

$$T_{lc-on}(\lambda) = 1 - \frac{\sin^2[\theta(1+u^2)^{1/2}]}{(1+u^2)}$$

Where:

$$u = \frac{\pi d_{lc} \Delta n(\lambda)}{\theta \lambda}$$

$\theta$  = twist angle in radians

$d_{lc}$  = cell gap

$$\Delta n(\lambda) = n_e(\lambda) - n_o(\lambda)$$

$n_e(\lambda)$  = extra-ordinary refractive index of LC

$n_o(\lambda)$  = ordinary refractive index of LC

$T_{xp}(\lambda)$  = transmission of crossed polarizers

### An Simplified Colorimetric Model for Binary Color LCDs Viewed On-Axis

A great deal of colorimetric/photometric analysis and optimization for LCDs can be accomplished with a reduced optical model for binary or bi-level displays viewed normal to the display surface. We have recently developed a simplified colorimetric model for binary LCDs and have applied the model successfully to the development of several prototype color LCDs.<sup>7</sup> While this reduced model does not allow for intermediate LC cell voltage states or estimates for off-axis directions of light propagation, it does enable efficient spectral tuning of the illumination source, LC parameters and principle LCD material layers. The basic equations for the SPDs of red LCD pixel elements in both the on- and off-states are given in Equation (5). Similar equations are required for the pixel elements of the other primary colors.

$$R_{on}(\lambda) = S(\lambda) T_{p-ent}(\lambda) T_{g-ent}(\lambda) T_{lc-on}(\lambda) \\ \times T_{red-f}(\lambda) T_{g-exit}(\lambda) T_{p-exit}(\lambda) T_{oe}(\lambda)$$

$$R_{off}(\lambda) = S(\lambda) T_{p-ent}(\lambda) T_{g-ent}(\lambda) T_{lc-off}(\lambda) \\ \times T_{red-f}(\lambda) T_{g-exit}(\lambda) T_{p-exit}(\lambda) T_{oe}(\lambda)$$

Where:

$S(\lambda)$  = SPD of illumination source

$T_{g-ent}(\lambda)$  = transmission of entrance glass  
(w/ITO and alignment layer) (5)

$T_{p-ent}(\lambda)$  = transmission of entrance polarizer

$T_{lc-on}(\lambda)$  = as defined in Equation (4)

$T_{lc-off}(\lambda)$  = as defined in Equation (4)

$T_{x-f}(\lambda)$  = transmission of color filter

$T_{g-exit}(\lambda)$  = transmission of exit glass

$T_{p-exit}(\lambda)$  = transmission of exit polarizer

$T_{oe}(\lambda)$  = transmission of other optical elements

Having calculated the SPDs of the LCD primary color pixels, we can now transform these quantities into CIE tristimulus values<sup>8</sup> and calculate the luminance of the primary color pixels. Again, here we calculate the

$$X_{r-on} = \int_{380}^{780} R_{on}(\lambda) \bar{x}(\lambda) d(\lambda) , X_{r-off} = \int_{380}^{780} R_{off}(\lambda) \bar{x}(\lambda) d(\lambda) \\ Y_{r-on} = \int_{380}^{780} R_{on}(\lambda) \bar{y}(\lambda) d(\lambda) , Y_{r-off} = \int_{380}^{780} R_{off}(\lambda) \bar{y}(\lambda) d(\lambda) \\ Z_{r-on} = \int_{380}^{780} R_{on}(\lambda) \bar{z}(\lambda) d(\lambda) , Z_{r-off} = \int_{380}^{780} R_{off}(\lambda) \bar{z}(\lambda) d(\lambda) \\ L_{r-on} = 683 Y_{r-on} \quad L_{r-off} = 683 Y_{r-off}$$

Where:

$\bar{x}$ ,  $\bar{y}$ ,  $\bar{z}$  = CIE 1931 color matching functions

$L_{x-xx}$  = luminance in cd/m<sup>2</sup>

(6)

tristimulus values of the red pixel elements only. Similar calculations are required for the other primary color pixel elements. Finally, we must calculate a weighted combination of the pixel element tristimulus values to convert these quantities to space-average tristimulus values. The space-average values enable us to account for the aperture ratio of the display, the color pixel mosaic and the non-zero luminance or "leakage" for off-state pixels.

$$\begin{aligned} X_{r-sa} &= A_r [(R_a X_{r-on}) + (G_a X_{g-off}) + (B_a X_{b-off})] \\ Y_{r-sa} &= A_r [(R_a Y_{r-on}) + (G_a Y_{g-off}) + (B_a Y_{b-off})] \\ Z_{r-sa} &= A_r [(R_a Z_{r-on}) + (G_a Y_{g-off}) + (B_a Z_{b-off})] \\ L_{r-on-sa} &= 683 Y_{r-sa} \end{aligned}$$

$$\begin{aligned} X_{g-sa} &= A_r [(R_a X_{r-off}) + (G_a X_{g-on}) + (B_a X_{b-off})] \\ Y_{g-sa} &= A_r [(R_a Y_{r-off}) + (G_a Y_{g-on}) + (B_a Y_{b-off})] \\ Z_{g-sa} &= A_r [(R_a Z_{r-off}) + (G_a Y_{g-on}) + (B_a Z_{b-off})] \\ L_{g-on-sa} &= 683 Y_{g-sa} \end{aligned}$$

(7)

$$\begin{aligned} X_{b-sa} &= A_r [(R_a X_{r-off}) + (G_a X_{g-off}) + (B_a X_{b-on})] \\ Y_{b-sa} &= A_r [(R_a Y_{r-off}) + (G_a Y_{g-off}) + (B_a Y_{b-on})] \\ Z_{b-sa} &= A_r [(R_a Z_{r-off}) + (G_a Y_{g-off}) + (B_a Z_{b-on})] \\ L_{b-on-sa} &= 683 Y_{b-sa} \end{aligned}$$

Where:

$A_r$  = display aperture ratio

$R_a, G_a, B_a$  = active area for R, G, and B pixels

$X_{*-sa}, Y_{*-sa}, Z_{*-sa}$  = space-average tristimulus values

To evaluate the accuracy of our reduced LCD colorimetric model, we compared the modeled space-average chromaticity coordinates of the display primaries and white point for an early color LCD prototype with spectro-radiometric measurements of the assembled display. The display was an active-matrix color LCD operated in the NW mode. The approximate display active area was 8.64 cm x 7.37 cm and a RGB delta-triad mosaic of color filters was used. For this early prototype, a standard HCF lamp was used as an illumination source and thus did not contain a tri-phosphor blend which was optimized for the thin-film color filters or LC parameters. A comparison of the modeled and measured chromaticity

coordinates for this color LCD, shown in Figure 5, reveals a close correspondence between predicted and measured colors. A small discrepancy is evident for the G primary, which also results in a small error for the white point. In general, small errors of this nature can often be attributed to slight changes in material characteristics and/or geometry occurring during fabrication and assembly of the completed display. The color gamut of a typical CRT monitor with P-22 phosphors is shown in Figure 5 to provide a color performance reference.

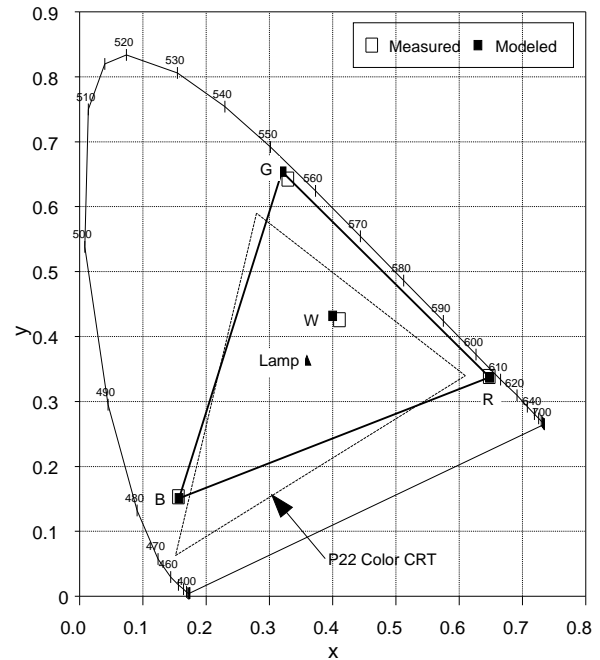
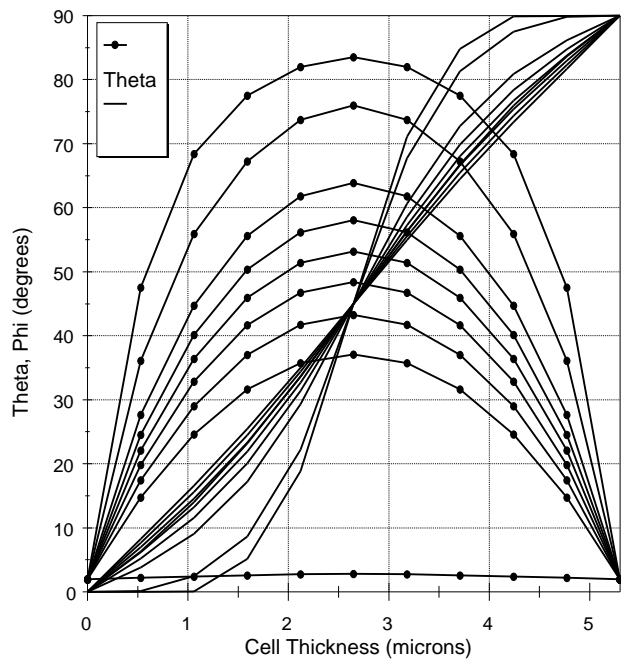
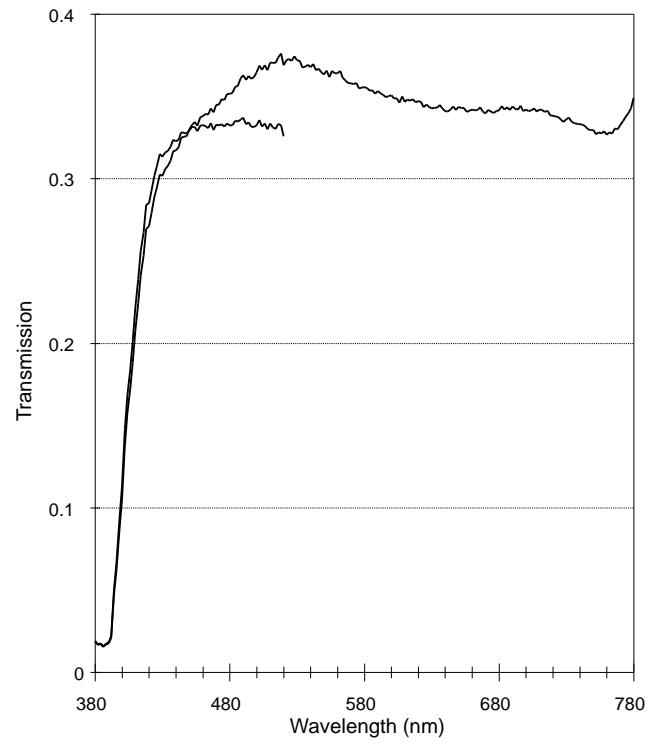
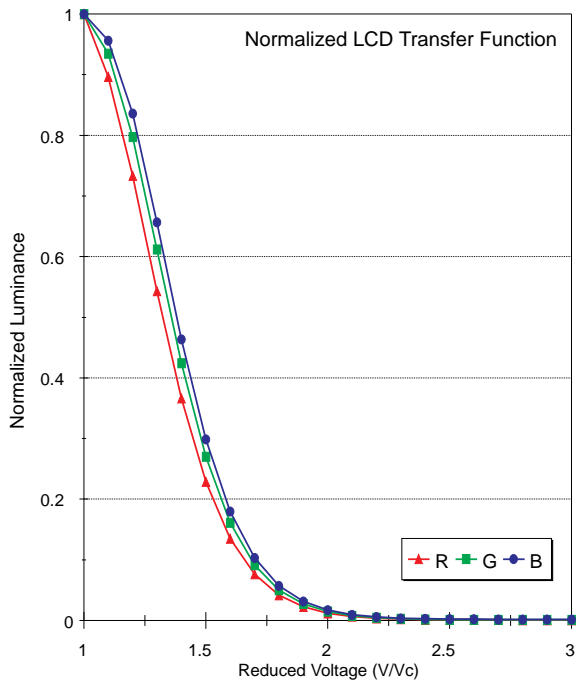


Figure 5. A comparison of modeled and measured chromaticity coordinates for an early prototype color LCD

### Voltage-Controlled Gray Scale and Off-Axis Viewing in LCDs

For both voltage-controlled gray scale and off-axis viewing, the light path through the LC layer "sees" a different birefringence than in the fully voltage-saturated, on-axis situation.<sup>4,9</sup> This is due to the fact that the angles at which the light path intercepts the anisotropic LC molecules vary as a function of LC cell voltage and viewing angle. This in turn results in different degrees of stimulation of the ordinary and extraordinary modes of the LC causing varying degrees of phase difference between the two polarization components, different polarization states at exit from the LC cell, and resulting







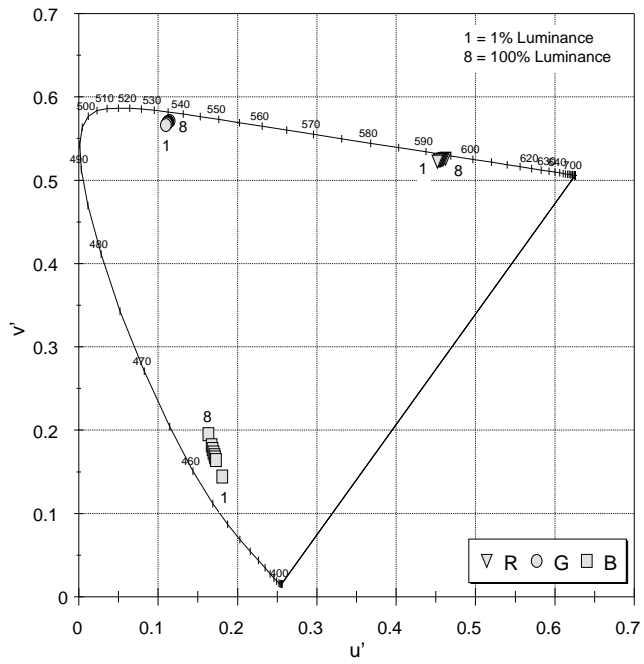
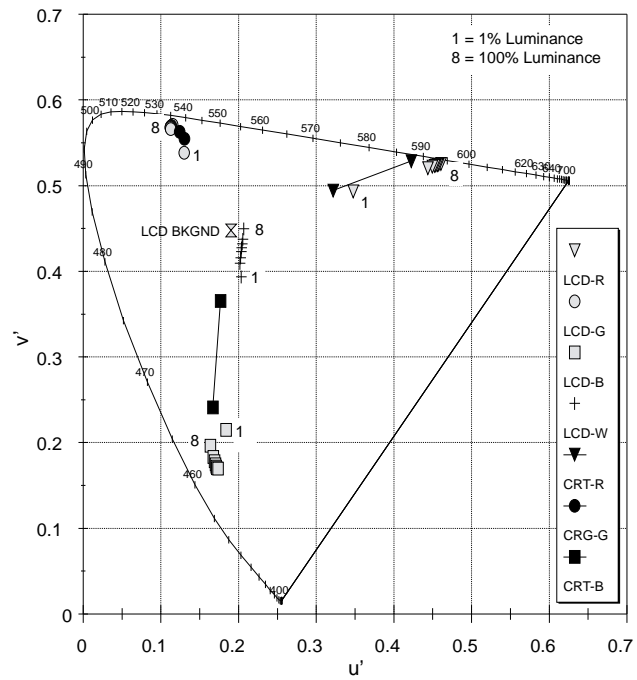


Figure 9



## References

- (1) Collings, P. J. (1990). *Liquid Crystals: Nature's Delicate Phase of Matter*. Princeton, New Jersey: Princeton University Press.
- (2) Penz, P. A. (1985). Nonemissive displays. In L. E. Tannas (Ed.), *Flat-Panel Displays and CRTs*. New York: Van Nostrand Reinhold Company, 415-457.
- (3) Scheffer, T., and Nehring, J. (1990). Twisted nematic and supertwisted nematic mode LCDs. In B. Bahadur (Ed), *Liquid Crystals: Applications and Uses, Volume I*. New Jersey: World Scientific Publishing Company, 231-274.
- (4) Scheffer, T., and Nehring, J. (1992). Twisted-nematic (TN) and super-twisted nematic LCDs. *Society for Information Display Seminar Lecture Notes*, Volume I, M1/1-1/52.
- (5) Klinger, D. S., Lewis, J. W., and Randall, C. E. (1990). *Polarized Light in Optics and Spectroscopy*. Boston: Academic Press, Inc.
- (6) Gooch, C. H., and Tarry, H. A. (1975). The optical properties of twisted nematic liquid crystal structures with twist angles  $\leq 90^\circ$ . *Journal of Applied Physics*, 8, 1575-1584.
- (7) Silverstein, L. D. (1991). *Description of an On-Axis Colorimetric/Photometric Model for Twisted-Nematic Color Liquid Crystal Displays*. Unpublished technical report for the NASA/ARPA Visual Display Engineering and Optimization System (ViDEOS) project.
- (8) Wyszecki, G., and Stiles, W. S. (1982). *Color Science: Concepts and Methods, Quantitative Data and Formulae, 2nd Edition*. New York: John Wiley & Sons, Inc.
- (9) Yariv, A., and Yeh, P. (1984). *Optical Waves in Crystals*. New York: John Wiley & Sons, Inc.
- (10) Yeh, P. (1982). Extended Jones matrix method. *Journal of the Optical Society of America*, 72, 507-513.
- (11) Ong, H. L. (1991). LCD modeling by  $2 \times 2$  and  $4 \times 4$  propagation matrix methods and by generalized geometrical optics approximation. *Proceedings of the 11th International Display Research Conference*, 1-5.
- (12) Lien, A. (1990). Extended Jones matrix representation for the twisted-nematic liquid-crystal display at oblique incidence. *Applied Physics Letters*, 57, 2767-2769.
- (13) Berreman, D. W. (1973). Optics in smoothly varying anisotropic planar structures: Application to liquid-crystal twist cells. *Journal of the Optical Society of America*, 63, 1374-1380.
- (14) Berreman, D. W. (1972). Optics in stratified and anisotropic media. *Journal of the Optical Society of America*, 62, 502-510.
- (15) Wohler, H., Haas, G., Fritsch, M., and Mlynski, D. A. (1988). Faster  $4 \times 4$  matrix method for uniaxial inhomogeneous media. *Journal of the Optical Society of America*, 5, 1554-1556.
- (16) Berreman, D. W. (1983). Numerical modeling of twisted nematic devices. *Philosophical Transactions of the Royal Society of London*, 309, 203-216.
- (17) Fiske, T. G., & Silverstein, L. D. (1993). Characterization of viewing-angle dependent colorimetric and photometric performance of color LCDs. *Society for Information Display Technical Digest*, 565-568.
- (18) Martin, R. A., Chuang, H., Steemers, H., Allen, R., Fulks, R., Stuber, D., Lee, D., Young, M., Ho, J., Nguyen, M., Meuli, W., Fiske, T., Bruce, R., Thompson, M., Tilton, M., and Silverstein, L. D. (1993). A 6.3 million pixel AMLCD. *Society for Information Display Technical Digest*, 704-707.
- (19) Silverstein, L. D., Krantz, J. H., Gomer, F. E., Yeh, Y., & Monty, R. W. (1990). The effects of spatial sampling and luminance quantization on the image quality of color matrix displays. *Journal of the Optical Society of America A*, 7, 1955-1968.